Obestatin increases the regenerative capacity of human myoblasts transplanted intra-muscularly in an immunodeficient mouse model

Icía Santos-Zas, Elisa Négroni, Kamel Mamchaoui, Carlos S Mosteiro, Rosalía Gallego, Gillian Butler-Browne, Yolanda Pazos, Vincent Mouly, Jesus P Camiña

HAL Id: hal-01961188

https://hal.sorbonne-universite.fr/hal-01961188v1

Submitted on 19 Dec 2018

Obestatin increases the regenerative capacity of human myoblasts transplanted intra-muscularly in an immunodeficient mouse model: proliferation, migration and differentiation

Icia Santos-Zas[1], Elisa Negroni[2], Kamel Mamchaoui[2], Carlos S Mosteiro[1], Rosalia Gallego[3], Gillian S. Butler-Browne[2], Yolanda Pazos[4], Vincent Mouly[2,*], Jesus P Camiña[1,*]

(1) Laboratorio de Endocrinología Celular, Instituto de Investigación Sanitaria de Santiago (IDIS), Complejo Hospitalario Universitario de Santiago (CHUS), Servicio Gallego de Salud (SERGAS); Santiago de Compostela, Spain.
(2) Sorbonne Universités, UPMC Univ Paris 06, INSERM UMRS974, Center for Research in Myology, 47 Boulevard de l'hôpital, 75013 Paris, France.
(3) Departamento de Ciencias Morfológicas, Universidad de Santiago de Compostela; Santiago de Compostela, Spain.
(4) Laboratorio de Patología Digestiva, IDIS, CHUS, SERGAS; Santiago de Compostela, Spain.

Short title: Obestatin stimulates human myoblast engraftment

*To whom correspondence should be addressed:

Vincent Mouly, PhD. Institut de Myologie, INSERM, and Sorbonne Universités, Université Pierre et Marie Curie, Paris, France. E-mail: vincent.mouly@upmc.fr

Jesus P. Camiña, PhD. Laboratorio de Endocrinología Celular. IDIS. Hospital Clínico Universitario de Santiago. Trav. Choupana s/n. 15706 Santiago de Compostela. Spain. E-mail: jesus.perez@usc.es

ABSTRACT

Although cell-based therapy is considered as promising method aiming at treating different muscular disorders, little clinical benefit has been reported. One of major hurdles limiting the efficiency of myoblast transfer therapy is the poor survival of the transplanted cells. Any intervention upon the donor cells focused at enhancing in vivo survival, proliferation and expansion is essential to improve the effectiveness of such therapies in regenerative medicine. In the present work, we investigated the potential role of obestatin, an autocrine peptide factor regulating skeletal muscle growth and repair, to improve the outcome of myoblast-based therapy by xenotransplanting primary human myoblasts into immunodeficient mice. The data proved that short *in vivo* obestatin treatment of primary human myoblasts not only enhances the efficiency of engraftment but also facilitates an even distribution of myoblasts in the host muscle. Moreover, this treatment leads to a hypertrophic response of the human-derived regenerating myofibers. Taken together, the activation of the obestatin/GPR39 pathway resulted in an overall improvement of the efficacy of cell engraftment within host's skeletal muscle. These data suggest considerable potential for future therapeutic applications and highlight the importance of combinatorial therapies.

INTRODUCTION

Cell-based therapy is considered to be one of the innovative methods aiming at treating different muscular disorders (1,2). Cell therapy is based on the delivery of precursor cells, autologous or heterologous, that will contribute to the regeneration of muscle fibers and tissue repair. This type of restorative therapy has the potential to establish genetically corrected myofibers and reverse the pathological phenotype. The fundamental requirements for the ideal cell candidate are related their myogenic potential, their homing capacities to sites of degeneration, and their motility in the target tissue. Furthermore, their isolation and amplification must be transferable under clinical conditions, preferably in an autologous context. Several cell therapy strategies have been tested using different types of cells with a myogenic potential and derived from muscle (satellite cells/myoblasts or muscle derived stem cells), vessels (pericytes and their progeny mesoangioblasts), bone marrow, blood, or embryonic tissues, including, recently, induced pluripotent stem cells (reviewed in 1,3,4). However, the data obtained from these studies resulted in suboptimal, although promising, effectiveness in restoring functional skeletal muscle tissue. First, the availability of an adequate number of stem cells to transplant constitutes an important challenge. This includes issues related to the harvesting from donors or from the same patient, genetic correction in case of autologous transplant, large-scale amplification in clinical conditions, maintenance of a myogenic potential prior to transplantation, and their compatibility with the host immune system. Once implanted, the lack of efficiency and survival of the transplanted cells remains a major hurdle for clinical application. Moreover, for diseases targeting a large number of muscles, their complexity and distribution throughout the body adds to the difficulties of delivering cells to muscles with restricted accessibility (1-3,5,6).

Myoblasts were the first candidate cell to be tested for cell therapy. Myoblasts are well-characterized physiological progenitors, for which isolation and expansion is feasible *in vitro*. Several studies have been successfully carried out in mice, showing that injected myoblasts are

able to participate to muscle regeneration (7) and restore the missing protein dystrophin in the mdx mouse, a widely used animal model of Duchenne muscular dystrophy (DMD) (8-13). However, the results of the first clinical trials in DMD patients were rather disappointing (14-16). Among the main reasons, the poor survival of cells, their lack of dispersion from the injection site and immunological rejection by the host have been proposed as potentially hampering any clinical benefit. Several studies have indicated that the vast majority of injected murine myoblasts die during the first hours following transplantation (17,18). The reasons for this early death are poorly understood and may be due to apoptosis, necrosis, anoıkis or non-specific immune destruction. Furthermore, the lack of cell survival was also observed in immunodeficient or immunosuppressed animals, illustrating that it is independent of any event related to the host's adaptive immune response (19). It was demonstrated that muscle damaging or irradiation improved the migration capacities of myoblasts (9,20), but such protocol is not clinically applicable. In fact, grafted myoblasts do migrate, but in a manner most closely associated with their physiological function to support myofiber regeneration rather than in one ideally suited to facilitate their transplantation as a potential therapy (21,22). It is well known that myoblasts migrate in response to signals deriving both from damaged fibers and infiltrating cells (23). In clinical settings, cell repartition was improved by innovative systems of injection (24,25). This protocol remains applicable to small and accessible muscles (e.g. thenar eminence, extensor digitorum or even biceps brachii) in DMD patients, or in the context of autologous cell transplantation for localized tissue repair in less extended diseases such as oculopharyngeal muscular dystrophy (26).

Several research groups have developed studies to improve the comprehension of the biology of these satellite cells such as their heterogeneity or their niche (27). Recent studies involving purification of satellite cells or sub-populations and implantation without any *in vitro* amplification (28-30) or implantation of one single intact myofiber (31) in mice have shown that cells nearer to satellite cell state or even still within their niche can robustly contribute to muscle repair. Particularly, the implantation of single fibers was by far the most efficient

procedure in terms of efficiency of participation in host's regeneration. In fact transplantation in dystrophic mouse muscles of a single muscle fiber that contained as few as seven satellite cells led to an increasing number of new satellite cells that in turn generated more than 100 new muscle fibers (31). Although reasons for this increased efficiency are not yet fully understood, this is a much more efficient way to generate new muscle fibers than transplantation of cultured satellite cells, in which normally the number of donor-derived new fibers that are generated is several orders of magnitude less than the number of injected cells. These results open new avenues for research on cell transplantation, based on comparisons between cultured and uncultured cells. Despite the promising value of this approach, this is not yet applicable in clinical situations, where a massive amplification of donor cell is still required, particularly in autologous trials.

In spite of progress made, significant gaps remain in the knowledge of areas such as survival, proliferation and migration of transplanted human myoblasts. The development of xenotransplantation strategies in immunodeficient preclinical mouse models allowed to analyze human myoblast behavior and the regulation of key biological events occurring in the host muscle to design rational strategies to improve grafting. Among them, recent studies demonstrated that a significant portion of grafted human myoblasts survives and engrafts host muscle, and although a cell death peak is noted, it seems far less than for murine myoblasts (32). Interestingly, *in situ* proliferation of human myoblasts was observed in the first days post-transplantation that was able to compensate for the loss of cells occurring after injection. Furthermore, the migration of grafted human myoblasts was limited to the same time window after transplantation, after which proliferation is downregulated and grafted myoblasts start to differentiate *in situ*, suggesting that proliferation, migration, and differentiation are tightly linked and that modifying one of these three processes has an impact on the others. Thus, insights into the molecular and cellular mechanisms regulating myoblast activation, proliferation and/or differentiation should allow to optimize conditions to improve the regenerative potential of amplified myoblasts. p38 was recently identified as a determining

switch to promote differentiation of satellite cells (33). Thus, reversible pharmacological inhibition of p38 in cultured human satellite cells resulted in a gene expression program consistent with the promotion of human satellite cells self-renewal, and it allowed for expansion of a population *ex vivo* with enhanced self-renewal and engraftment potential. Recently, it was also proposed that compounds stimulating the expansion of the satellite cell pool, such as recombinant Wnt7a, improve motility and engraftment leading to significantly improved muscle function (34). These results highlight the need to develop strategies to reduce early cell death and promote proliferation so as to limit the number of cells required for successful engraftment.

Autocrine factors that can regulate the activation and proper differentiation of myoblasts would be particularly useful to improve the outcome of myoblast-based therapies. In this context, we have recently reported that obestatin, a 23-amino acid peptide derived from a polypeptide called preproghrelin, is involved in muscle regeneration, exerting an autocrine function to control the myogenic differentiation program (35). Obestatin regulates multiple steps of myogenesis: myoblast proliferation, cell cycle exit, differentiation and recruitment to fuse and form multinucleated hypertrophic myotubes (36). This action is coordinated by the interplay between G-protein-dependent and ß-arrestin-dependent mechanisms (37). The obestatin-associated mitogenic action is determined by G-protein-dependent activation defining the intricate pathways related to the ERK1/2 and JunD axis; and, the transactivation of EGFR through the β-arrestin signal complex determines the cell cycle exit, the development and the progression of differentiation through a kinase hierarchy determined by the Akt, CAMKII, c-Jun and p38 axes. Added to the functional features, the chemical/biochemical properties and the existence of an easily available 23-amino acid peptide with high dispersal profile in skeletal muscle (36), undoubtedly facilitate its use as a therapeutic agent.

In this work, we investigated the potential of obestatin to improve the outcome of myoblast-based therapy by xenotransplanting primary human myoblasts into immunodeficient mice. Our results showed that a short *in vivo* treatment of human myoblasts with obestatin not only

enhances the efficiency of engraftment but also facilitates an even distribution of myoblasts in the host muscle. Moreover, this treatment leads to a hypertrophic response of the human-derived regenerating myofibers. Our observations suggest obestatin as a pharmacological mean to improve the outcome of myoblast-based therapy, which might be beneficial for future regenerative therapies of skeletal muscle.

RESULTS

Functional validation of the obestatin/GPR39 system in human primary myoblasts. The expression of the obestatin/GPR39 system was assessed in human primary myoblasts during myogenesis. Upon reaching confluence, serum and additives were withdrawn to induce the differentiation from proliferative myoblasts into terminally differentiated myotubes. As shown in Figure S1a, obestatin is not expressed in primary myoblasts but is up-regulated in differentiated myotubes (6-day differentiation period). However, GPR39 was detected in both myoblasts and myotubes (Fig. S1a). In human primary myoblasts, obestatin (10 nM, 5 min) activated MAPKs [ERK1/2, c-Jun/JunD, and p38], Akt, and CAMKII signaling pathways (Fig. S1b). These kinase hierarchies are decoded by the myogenic effectors that execute different phases of the differentiation process in response to the obestatin/GPR39 system (37). In the context of obestatin-induced activity, obestatin increased mitogenic event in a dose–effect relationship with maximal effect at 10 nM obestatin in GM (proliferating conditions; Fig. S1c). To assess the activity of obestatin as a promoter of the differentiation process, primary myoblasts were switched to DM supplemented with obestatin at 10 nM for 6 days. Immunoblot analyses revealed enhanced protein level of MHC when compared with control cells (DM for 6 days; Fig. S1d). The myotube areas were larger in the obestatin-treated cells (DM + 10 nM obestatin; 3401 ± 33 μm^2) as compared to control conditions (DM; 168 ± 36 μm^2) at 6 days after differentiation. To quantify myoblast fusion, we calculated the fusion index by expressing the number of nuclei within MHC$^+$ myotubes with ≥ 3 nuclei as a percentage of the total nuclei. The fusion index was significantly higher in the obestatin-treated cells compared with untreated control cells (47.0 ± 0.8 and $33.4 \pm 1.2\%$, respectively; Fig. S1c). Nuclear number analysis revealed that the percentage of myotubes with >30 nuclei was significantly higher in obestatin-treated cells compared with control cells (Fig. S1c). Thus, obestatin regulated multiple steps of myogenesis, including myoblast proliferation, differentiation and recruitment to fuse and form multinucleated hypertrophic myotubes.

Mitogenic effect *in vivo* of obestatin in regenerating muscle. To test the obestatin effect on human cells within the murine recipient muscle, we transplanted 5×10^5 myoblasts cells into freeze damaged TA muscle followed by obestatin delivered via intramuscular injection every 24 hours up to 5 consecutive days (Fig. 1a). The expression of ki67, (a protein expressed in all cell-cycle phases except G_0), was analyzed on cross sections of TA muscles grafted with human cells, in parallel with the detection of human Lamin A/C. At 24 hours post-transplantation, the number of human Ki67$^+$ cells (Lamin A/C$^+$ cells) in grafted TAs was not significantly different whether they had been treated with obestatin or not (17.6 ± 3.5 and 19.3 ± 2.9 ki67$^+$ cells, respectively; Fig. 1b). 5 days post-transplantation there was a 38% decline in the number of human Ki67$^+$ cells in the untreated animals. By contrast, the analysis of Ki67 expression in obestatin-treated mice showed an 80% increase in the number of human Ki67$^+$ cells compared untreated recipients (21.4 ± 2.2 and 11.9 ± 0.7 ki67$^+$ cells, respectively; Fig. 1b), thus maintaining the levels of proliferating cells observed at 24 hours post-transplantation. An analysis of phospho-histone-3 (S10) (pH3) expression, a marker of the late G2- and M-phase of the cell cycle, demonstrated an 114% increase in pH3$^+$ human cells in the obestatin-treated group as compared to the control group at 24 hours post-transplantation (10.4 ± 1.0 and 4.9 ± 0.9 pH3$^+$ cells, respectively; Fig. 1c). Despite the decline in the relative numbers of pH3$^+$ cells at 5 days post-transplantation, the number of human pH3$^+$ cells was double in the obestatin-treated group than in the control group (5.6 ± 1.1 and 2.8 ± 0.6 pH3$^+$ cells, respectively; Fig. 1c). Calculation of the apoptotic cells from TUNEL labeling showed that obestatin treatment significantly attenuated the number of apoptotic nuclei at 5 days of transplantation (15.0 ± 2.4 and 1.0 ± 0.4 cells, respectively; Fig. 1d). Furthermore, the expression of cleaved caspase-3 (activated caspase-3) decreased in human cells in the obestatin-treated group as compared to the control group at 5 days post-transplantation (Fig. 1e). Thus, the increased expression of Ki67 and pH3 proteins, together with reduced rates in apoptosis, supports that the proliferation of muscle precursors is stimulated by the obestatin treatment decreasing, at least in part, the loss of injected cells.

Obestatin treatment increases cell migration *in vitro* and *in vivo*. We next investigated whether the activation of obestatin/GPR39 system could modulate human cell migration *in vivo*, while colonizing the recipient´s tissue. In order to do this, we measured the area occupied by the human cells on transverse sections along the entire length of the muscle at the different time points described above. At 24 hours post-transplantation, the area occupied by the human cells did not show significant differences between control and obestatin-treated muscles (422.5 ± 38.9 and 369.8 ± 124.0 μm^2, respectively; Fig. 2a). At 5 days post-transplantation, the area occupied by human cells within regenerating muscle treated with obestatin was increased by 132% as compared to untreated muscle (1245 ± 239.6 and 536.3 ± 110.2 μm^2, respectively; Fig. 2a). Importantly, 21 days post-transplantation (i.e.16 days after the last obestatin administration), the area occupied by human cells in obestatin-treated muscles was 59% greater compared to untreated group (1833 ± 241.2 and 1146 ± 100.7 μm^2, respectively; Fig. 2a). Similar results were obtained when relative areas, i.e. total area/human cell number, or the cell number per unit area were compared (Fig. 2a). These results ruled out the possibility that the increased area might be related to the proliferation response.

The effect of obestatin on cell motility was further tested in scratch assays. To exclude a bias arising from different rates of proliferation, we treated the human primary cells with mitomycin-C (15 $\mu g/mL$; 2-hours), a DNA replication inhibitor. Addition of obestatin (10 nM) to the culture medium increased the migration of human cells by ~28.7 and ~44.6% when compared to untreated control at 24- and 48-hours, respectively (Fig. 2b). To identify potential effectors of obestatin/GPR39 signaling, we investigated the requirement of Disheveled 2 protein (Dvl2). Despite primary cells provided a valuable complement to *in vivo* experiments, their *in vitro* culture requirements limited the efficacy of siRNA transfection [siRNA-mediated knockdown of Dvl2 (si-Dvl2); 8.7 ± 2% reduction relative to scrambled siRNA (si-control)]. To achieve maximum efficacy, siRNA experiments were carried out in the hTERT/cdk4 immortalized human myoblasts (KM155C25 clone 48; see Material and Methods for details), a reliable and stable

immortalized cell line derived from primary cells that retain the characteristics of non-senescent primary line, i.e. in vitro and in vivo differentiation, with extended proliferative lifespan (38). siRNA-mediated knockdown of Dvl2 [$60.4 \pm 0.5\%$ reduction relative to scrambled si-control] significantly prevented obestatin-mediated migration in scratch assays when compared with the si-control (Fig. 2c). The small GTPases, Rac1 and Rho, have also been proposed to be involved in obestatin-mediated cell migration. Indeed, obestatin significantly increased the activation of Rho (160% relative to si-control; Fig. 2d) while it had no significant effect on active Rac1 (Fig. 2D). si-Dvl2 significantly reduced by 73% the activation of Rho in obestatin-stimulated cells when compared with the si-control (Fig. 2d). We conclude that obestatin/GPR39 increase the migration of human cells in the host muscle through activation of Dvl2 and the small GTPase Rho.

Obestatin promotes differentiation of muscle precursors *in vivo*. We analyzed the expression of myogenin, a key myogenic regulatory factor, which is also a marker of early skeletal muscle cell differentiation (39) as well as of MHC, a marker of terminal differentiation (40). As determined by immunostaining for myogenin on muscle sections, obestatin treatment tends to increase the number of myogenin$^+$ cells although this is not significant when compared to controls at 5 days post-transplantation (20.4 ± 1.0 and 15.9 ± 2.9 % myogenin$^+$ cells, respectively; Fig. 3a). When the expression of MHC was evaluated in the injected human muscle cells at the same time point, the treated-to-control ratios showed a 33% decrease in MHC$^+$ cells (47.0 ± 2.0 and 70.0 ± 1.0 % MHC$^+$ cells, respectively; Fig. 3b). However, the cross-section areas of fibers with centrally located human Lamin A/C$^+$ nuclei (i.e. regenerating fibers) were 289.8% larger in obestatin-treated mice (752.0 ± 63.0 μm^2) than in control mice (193.0 ± 14.0 μm^2) at 5 days post-transplantation (Fig. 3b). Furthermore, the number of human myonuclei per regenerating myofiber was significantly increased by 105% in the obestatin-treated group (2.1 ± 0.07 cells) when compared with the control muscles (1.0 ± 0.01 cells; Fig. 3b). Thus, myogenin and MHC expression excluded rapid differentiation of the transplanted human cells and correlates with activation of the proliferating stage. Despite the fact that there

is fewer fibers with human nuclei, obestatin treatment was accompanied by an increase in fiber hypertrophy and in myonuclear content.

Obestatin increase the regenerative capacity of human myoblasts *in vivo*. To assess the overall efficiency of *in vivo* engraftment of human cells in a regenerated muscle in the presence of obestatin/GPR39 activation, TA muscles were immunostained for human Lamin A/C and mouse laminin at 21 days post-transplantation. The number of myofibers containing human nuclei was increased by 112% in obestatin-treated compared to control muscles (193.7 ± 19.2 and 91.0 ± 20.0, respectively; Fig. 4a). Furthermore, the total number of human cells engrafted into mouse myofibers was 135% greater in the obestatin-treated muscles than in the control group (386.7 ± 52.5 and 164.3 ± 46.6 human grafted-cells, respectively; Fig. 4a). The participation of the injected cells in muscle regeneration was further quantified by counting the number of human spectrin$^+$ fibers per muscle section at 21 days post-transplantation. As shown in Figure 4B, obestatin increased by 1.8-fold the number of human spectrin$^+$ fibers. Related to the total number of fibers per muscle section, 15 ± 3 % spectrin$^+$ fibers were observed in obestatin-treated TA versus 8 ± 1 % in the control group. The analysis of cross-sectional areas showed that the treated-to-control ratio of all fibers (spectrin$^+$ and spectrin$^-$ fibers) was 16% larger in obestatin-treated mice (1605.0 ± 46.0 μm^2) than in control mice (1389.0 ± 40.0 μm^2) at 21 days post-transplantation, respectively (Fig. 4b). The cross-sectional areas of spectrin$^+$ fibers were 98% larger in obestatin-treated mice (2629.8 ± 172.0 μm^2) than in control mice (1327.9 ± 92.0 μm^2) with a shift of the muscle fiber size distribution towards major caliber fibers (Fig. 4c). However, cross-sectional areas of spectrin$^-$ fibers were similar in obestatin-treated mice (1440.9 ± 49.0 μm^2) compared to control mice (1397.9 ± 49.0 μm^2). Overall, these data demonstrate that obestatin globally enhanced the regenerative capacity of the injected cells, as shown by the increase in both the number of myofibers containing human nuclei and/or expressing human protein and the significantly increased size of the human-derived regenerated myofibers.

Once the differentiation process is triggered, myoblasts have a dual fate: while most commit to myogenic differentiation, there is a population that withdraws from the cell cycle and re-expresses markers of quiescent satellite cells, including Pax7. We investigated whether the obestatin/GPR39 system may also regulate this dual fate. To identify progenitor cells of donor origin, muscle sections were stained with antibodies against human Lamin A/C and Pax7 (Fig. 5). In representative sections, the number of $Pax7^+$ cells per 100 fibers, which include cells of both human and mouse origin (total $Pax7^+$ cells), was 50 ± 3 in control muscles, and the number of human $Pax7^+$/Lamin A/C^+ cells per 100 fibers was 8 ± 1, which accounts for $16 \pm 2\%$ of total $Pax7^+$ cells in the absence of treatment. By contrast, the numbers of total $Pax7^+$ and $Pax7^+$/ Lamin A/C^+ cells per 100 fibers were 107 ± 5 and 69 ± 8 in obestatin-treated muscles, respectively. This accounts for $65 \pm 10\%$ of total $Pax7^+$ cells. The numbers of $Pax7^+$/ Lamin A/C^- cells per 100 fibers (i.e. host satellite cells) were 42 ± 3 and 38 ± 11 in control and obestatin-treated muscles, respectively. To further determine whether donor-derived $Pax7^+$ cells were in the satellite cell position, triple labeling of human Lamin A/C, Pax7, and laminin was performed. Donor-derived $Pax7^+$ cells were located both in the satellite cell position (underneath the basal lamina of myofibers; Fig. 5) and outside the basal lamina. There were 1.0 ± 0.3 in control group and 14.8 ± 1.2 in obestatin group human $Pax7^+$/ Lamin A/C^+ cells per 100 fibers located inside the basal lamina. These data indicate that $21.4 \pm 1.7 \%$ of $Pax7^+$ donor cells are in the position of satellite cells, the remainder being undifferentiated interstitial myoblasts located outside the basal lamina. We further quantified the number of human cells that had not been incorporated into the muscle fibers but remained located in an interstitial position outside the basal lamina of the fibers This number was significantly larger for control compared to obestatin-treated muscles ($39 \pm 3\%$ and $18 \pm 4\%$ relative to total number of human cells, respectively).

Discussion

Although myoblast transfer therapy has appeared as promising from the results obtained in murine models, the results of clinical trials for DMD patients to date are disappointing, since little clinical benefit have been reported (1,41). The poor survival of the transplanted cells remains a major hurdle limiting its efficiency. Previous results have also shown that a reduced proliferation of the transplanted human myoblasts is correlated with their early differentiation within the host tissue (32). An analysis of the proliferation of human myoblast cells transplanted into regenerating muscles of immunodeficient mice using Ki67 or pH3 as markers of dividing cells, showed a limited *in vivo* amplification of the injected cells after engraftment. This reduced proliferation and early differentiation within the host tissue, was correlated to a limited migration of the transplanted human myoblasts within the host tissue. Any intervention upon the donor cells and/or the recipient's microenvironment focused at enhancing in vivo survival, proliferation and expansion before differentiation would be essential to improve the effectiveness of cell-based therapies in regenerative medicine. Obestatin, an autocrine factor regulating the function of myoblast pool and improving the ultimate efficiency of the engraftment, fulfill some of these requirements. Our results demonstrate that: 1) stimulation of proliferation of human myoblasts through the activation of the obestatin/GPR39 pathway delays myogenic differentiation, thus increasing the number of cells which can then colonize a much larger area within the recipient's muscle; 2) obestatin treatment results in increased cell migration through activation of Dvl2 and the small GTPase Rho; 3) obestatin-stimulated myoblasts maintain their ability to differentiate, since a higher number of myofibers containing human nuclei and/or expressing human proteins is found. Moreover, obestatin treatment leads to a hypertrophic response in the human-derived regenerating myofibers; and, 4) obestatin signaling enhances the capacity to reconstitute a satellite cell pool from transplanted cells, advocating their potential for long-term treatment of muscle diseases. Combined together, these

14

effects of the activation of the obestatin/GPR39 pathway result in an overall improvement of the efficacy of cell engraftment within host's skeletal muscle.

It was already shown that transplantation of these myogenic precursors in the presence of serum, which maintain the proliferative state of myoblasts *in vitro*, improved the outcome of myoblast transplantation (32). In agreement with these observations, we show that an exogenous induction of myoblast proliferation via obestatin stimulation has similar consequences on their participation to host's tissue, with the advantage of using a single molecule instead of serum which is clinically irrelevant. The fact that more cells are cycling and expressing markers of proliferation at 5 days post-transplantation clearly indicates that obestatin extends the phase of proliferation of implanted cells. Despite this extended proliferation, it should be noted that their myogenic potential is not compromised, since they can still be committed to differentiate after obestatin treatment as demonstrated by the number of myogenin^{+} human cells observed at day 5 post-engraftment. These observations support the hypothesis that self-renewal is a mechanism regulated by the obestatin/GPR39 system where myoblasts-derived myoblasts give rise to both differentiated cells and functional myoblasts. Further evidence for self-renewal has come from studies of myoblast transplantation into adult muscle, where neonatal myoblasts/satellite cell-derived myoblasts gave rise to both differentiated myonuclei and functional satellite cells (42,43). Observations on the dynamic expression of Pax7, MyoD, and myogenin in *ex vivo* cultured single myofibers are crucial to guiding satellite cells/myoblasts from an active to a quiescent state (44-46). While most of proliferating Pax7^{+}/MyoD[+] myoblasts differentiate into Pax7^{−}/MyoD[+]/myogenin^{+} cells, some Pax7^{+}/MyoD[+] myoblasts, repress MyoD expression preserving Pax7 expression and ultimately withdraw from the cell cycle. Future studies are needed to identify the regulatory mechanisms governing this process linked to obestatin/GPR39signaling.

In addition to efficient proliferation of the transplanted human cells, the efficiency to reconstitute the host skeletal muscle involves also extensive migration within the recipient's

muscle. Previous studies have shown that myoblasts have a very limited migration and remain confined at the injection site (32). Indeed, control engrafted cells only occupy a small volume of the muscle at 21 days post-injection. By contrast, obestatin clearly extended the dispersion and consequently the area occupied in the recipient's muscle during the same time. In agreement with these observations, our experiments with primary or immortalized myoblasts support that the enhanced tissue dispersion of obestatin-stimulated cells is due to an increased intrinsic migratory capacity at early time points after myoblast transplantation and does not involve induction of proliferation. Importantly, blocking Dvl2 signaling by siRNA transfection inhibited obestatin-induced cell migration, indicating that Dvl2 activation participates in the regulation of the myoblast migration. In our study, specific downregulation of Dvl2 signaling in immortalized myoblasts suppresses obestatin-induced activation of small GTPases Rho. These findings suggest a molecular pathway linking obestatin/GPR39 signaling with Dvl2/Rho in governing cytoskeletal architecture and cell motility (47,48).

At late stage of muscle regeneration, obestatin treatment increased the number of spectrin-expressing myofibers in the host muscle. Furthermore, the efficiency of the engraftment was ameliorated by the increased cross-sectional area of the newly formed muscle fiber that resulted from human cell fusion. This increase in both fusion and fiber size might be interpreted as a result of mitotic expansion of human cells, so that more cells can differentiate and participate to the repair of the tissue. However, we have already demonstrated that the muscle hypertrophic response to obestatin is not associated with the addition of new myonuclei via proliferation and further fusion (35-37). It should be considered that hypertrophy is strongly associated to Akt activation, a pathway that is activated by obestatin during the differentiation program and skeletal muscle regeneration (35-37). This pathway controls mechanisms of protein synthesis at several stages (e.g., translation capacity, translation efficiency) through the increase of specific mRNAs translation, which results in myotubes and fiber enlargement (49-51). Therefore, obestatin action is a highly coordinated process in which various signaling pathways converge

to activate specific gene expression programs associated to each stage of myofiber formation: proliferation, differentiation, fusion, and hypertrophic response.

On the whole, obestatin treatment increased the cross-sectional area of the human-derived regenerating myofibers with no significant effect found on mouse regenerating myofibers. Furthermore, obestatin did not modify host satellite cell population. Because of the hypertrophic effect of obestatin in murine skeletal muscle and its role in the expansion of satellite cells (36), these data seem disconcerting since the whole regenerating muscle is being treated. However, these results are consistent with the existence of a species-specific activity associated to obestatin because mice were treated with human obestatin. In fact, mouse and human obestatin exhibit clear conformational differences beyond their differences in primary structure (52). The mouse analogue adopts a distinct three-dimensional structure, which cannot activate human GPR39 (52). These structural differences are responsible for the different bioactivities observed. This species-specific activity allowed us to demonstrate the usefulness of exogenous induction of myoblast proliferation *in vivo* to improve the efficacy of engraftment. However, this property also provide indirect evidence that, if used clinically, host satellite cells can become activated by human-specific obestatin and contribute to muscle regeneration as grafted donor cells. In particular, endogenous satellite cells might outcompete the transplanted cells and give rise to regenerated sections of myofibers that contain, for example, no dystrophin within DMD patient muscles. Thus, the next important goal is to enhance donor cell response in relation to that obtained from host satellite cell. It is possible that an *ex vivo* treatment of human myogenic cells with obestatin is sufficient to enhance donor cell engraftment and tissue dispersion. Future experiments will investigate both how to regulate in a specific, proportionate manner the donor cells through the obestatin/GPR39 system, and the utility of modulating this system in vivo to augment the efficacy of engraftment muscle.

The ideal cell approach for muscle therapy must be capable of repopulating the precursor cell pool, providing an enduring source of regenerative cells for future muscle repair after injury.

Previous studies have shown that murine as well as human myoblasts were able to give rise to satellite cells after transplantation in mice (53-59). This is further supported by the present work in which transplanted myoblasts generate stem cell-like populations that reside in the satellite cell location, providing evidence for human stem cell self-renewal. Strikingly, this capacity was notably enhanced after obestatin treatment, increasing the number of human Pax7^{+} cells into the satellite cell compartment. Therefore, obestatin not only allows reconstitution of mature muscle fibers but also replenishes the muscle precursor pool by engrafted donor cells, thus seeding a reserve pool of cells that may be recruited for subsequent rounds of muscle repair. This observation supports the postulated hypothesis that the obestatin/GPR39 pathway can regulate cell assignment: dividing myoblast can either enter terminal differentiation or remain in a precursor state via self-renewal, involving withdrawal from the terminal myogenic program to maintain the satellite cell pool. This population of reserve cells retains the ability to reenter cell cycle and differentiate.

Overall, the present data validate the concept that any intervention upon the donor cells aiming at improving proliferation and migration should be done before differentiation of implanted cells. Furthermore, our work identifies a clinically relevant pharmacological mean to significantly improve the outcome of cell-based therapy for muscle diseases, highlighting the importance of combinatorial therapies. The proper activation and differentiation of transplanted cells via obestatin/GPR39 offer unique opportunities for muscle regenerative medicine.

Material and Methods

Materials. Human obestatin was obtained from California Peptide Research (Napa, CA, USA). Antibodies used are listed in Table S1. All other chemical reagents were from Sigma Chemical Co. (St. Louis, MO, US).

Animals. Rag2$^{-/-}$Il2rb$^{-/-}$ immunodeficient mice aged 2-3 months were used as recipients for human myoblast transplantation (60). Experimental procedures were performed in accordance with the legal regulations in France and with European Union ethical guidelines for animal research.

Primary human myoblasts. Human myoblasts were isolated from the semitendinosus muscle of a 25-year-old male in accordance with the French legislation on ethical rules, as described previously (61). The initial muscle biopsy was obtained anonymously through MyoBank, affiliated to EuroBiobank, in accordance with European recommendations and French legislation (approval reference AC-2013-1868), washed through two changes of DMEM medium (Lonza, Pontevedra, SP) and carefully microdissected under aseptic conditions to exclude fat and connective tissue. Cleaned muscle pieces were then cut into ~400 μm^3 cubes and plated onto FBS-washed 60 mm^2 dish for 1 hour. After microexplants attachment, growth medium [GM: Medium 99:DMEM (1:4, v: v; Lonza, Pontevedra, SP) supplemented with 20% FBS (v/v), 25 μg/μL fetuin, 5 ng/mL hEGF, 0.5 ng/mL bFGF and 50 μg/mL gentamycin (Invitrogen; Thermo Fisher Scientific, CO, USA)] was added. All cultures were performed at 37°C in a humid atmosphere containing 5% CO$_2$. Mononucleated cells migrating out of the explants were removed from the dish by using a 1.5% trypsin-0.04% ethylenediaminetetraacetic acid (EDTA) solution in PBS and then plated at a density of 2x103 cells/cm^2. The myogenic cell population was enriched using a CD56 magnetic bead sorting system (MACS; Miltenyi Biotec, Paris, France) according to the manufacturer's instructions. Briefly, cells were labeled with anti-CD56 (a specific marker of myoblasts) microbeads, and then separated in a MACS column

placed in a magnetic field. Purification was checked by immunochemistry using a desmin marker (62). All of the primary cell preparations used in this study, C25 cells, had a myogenic purity of at least ≥ 90%. The mean population doubling (MPD) was determined at each passage as described previously (38). Experiments were performed with C25 cells between 10 and 15 mean population doubling (38). Cell counting was carried out by means immunofluorescence using desmin as a marker for myoblasts and TOPRO®-3 (Thermo Fisher Scientific; Topro, fluorescent nuclear and chromosome counterstain) for nuclear staining. For differentiation into myotubes, C25 cells were cultured on Matrigel-covered glass coverslips in GM. At 80% confluence, GM was switched to differentiation medium [DM: DMEM or DMEM supplemented with obestatin 10 nM] for 5 days unless otherwise stated.

Cell preparation and myoblast transplantation. Mice were anesthetized by an intraperitoneal injection of 80 mg/kg of ketamine hydrochloride and 10 mg/kg xylasine (Sigma-Aldrich, St Louis, MO, USA) as described previously (63). Surgical procedures were performed under aseptic conditions and in accordance with the legal regulations in France and with European Union ethical guidelines for animal research. Primary myoblasts (C25 cells), grafted *in vivo* in this study had achieved 10-15 MPD, and were thus far from senescence (38, 64). Cells were trypsinized, centrifuged, and resuspended in DMEM. Before cell implantation, right TA muscles were subjected to three consecutive cycles of freeze/thawing by applying on the muscle surface exposed by opening the skin, a liquid nitrogen cooled metallic rod as described previously (32). Animals were assigned to one of two-matched experimental groups (n=10 per group): (i) obestatin-treated group and (ii) control group. Cell suspensions containing 5×10^5 myoblasts in DMEM or DMEM+obestatin (300 nmol/Kg body weight) were injected in a single injection site in the mid belly of the TA immediately after cryodamage. The skin was then closed using fine sutures. Obestatin treatment was prolonged 24-hours after cell transplantation injecting 20 µl of obestatin solution in DMEM (300 nmol/kg body weight) into the target muscles each 24 hours during 5 days following the protocol previously described (36). Control group was treated with 20 µl of DMEM under same conditions. Injections were performed

inserting the needle of a 0.3 mL/29 gauge syringe (Becton, Dickinson and Company, Franklin Lakes, NJ) for 1 mm in the distal part of the muscle. At 24 hours, 5 and 21 days after engraftment, mice were sacrificed (n=5 for each time point) and the TAs were dissected. In all experiments, the TAs were mounted in tragacanth gum (Sigma-Aldrich), and frozen in isopentane precooled in liquid nitrogen.

Cell culture and differentiation of human immortalized myoblasts. Immortal human myoblasts were derived from the C25 primary culture as previously described (38). Immortalized human myoblasts, KM155C25 Clone 48 (KM155C25 cells), were cultivated in GM containing Medium 199:DMEM (1:4, v/v; Lonza, Pontevedra, SP) supplemented with 20 % FBS (v/v), 25 µg/µL fetuin, 5 ng/mL hEGF, 0.5 ng/mL bFGF, 0.2 µg/mL dexamethasone (Sigma-Aldrich; MO, USA) and 50 µg/mL gentamycin (Invitrogen) as previously described (37,38). To confirm that immortalized cell line maintained their myogenic signature, the expression of several myogenic markers [desmin, neural cell adhesion molecule (N-CAM) and MyoD] was assessed in proliferating primary and immortalized cell line. In addition, the ability to differentiate into myotubes, using immunostaining with MF20 antibody, which recognizes all skeletal-muscle myosin heavy chains (MHC), was investigated. Differentiation into myotubes was initiated at 90 % confluence by switching to differentiation medium [DM; DMEM supplemented with obestatin and 50 µg/mL gentamycin (Invitrogen)] for 6 days. Immortalized cells retain the characteristics of the unmodified parental population (C25 cells) (38).

GST pull downs: Rac1/Rho activity assays. Active Ras-related C3 botulinum toxin substrate 1 (Rac1) and Ras homolog family member (Rho) pull-down and detection kits (Thermo Fisher Scientific, CO, USA) were used to perform Rac1 and Rho activation assays. In both cases, KM155C25 cells were washed in cold PBS and then lysed in equal volumes of 1X Lysis/Binding/Wash buffer (25 mM Tris-HCl, pH 7.5, 150 mM NaCl, 5 mM MgCl2, 1% NP-40 and 5% glycerol) with protease and phosphatase inhibitor mixtures (Sigma-Aldrich, Missouri, USA). Lysates were added into prewashed agarose glutathione beads and incubated for 90 min

at 4 °C with gentle rocking. GTP-bound Rac1 and GTP-bound Rho were affinity precipitated from cell lysates (300-500 μg of protein) using an immobilized GST fusion construct containing the p21-binding domain (PBD) of human p21-activated protein kinase 1 (Pak1) that binds to Rac1-GTP but not to Rac1-GDP and using an immobilized GST-fusion protein of the Rhotekin-binding domain (RBD) along with glutathione agarose resin to specifically pull down active Rho. The complexes were then subjected to immunoblot analysis using Rac1-specific antibody. Total cellular lysates were also separated by SDS-PAGE, and immunoblot blot analysis with anti-Rac1 and anti-Rho antibodies was done as a control for protein loading.

Small interfering RNA (siRNA) silencing assays. Chemically synthesized double-stranded siRNA duplexes targeting Dishevelled 2 (Dvl2) were selected from ON TARGETplus SMARTpool siRNA from Dharmacon (Thermo Fisher Scientific; Dvl2, GCUCAAAGCAGGC-CUGAUC, GGGAGACGAAGGUGAUUUA, CGCUAAACAUG-GAGAAGUA, CCACAAU-GUCUCUCAAUAU). An ON-TARGETplus nontargeting siRNA was used as a control. KM155C25 cells were transfected in suspension with Lipofectamine 2000 (Invitrogen). In short, siRNA is put in each well prior to transfection and combined with diluted Lipofectamine 2000 to form complexes in each well. Cells are added directly to the Lipofectamine 2000-siRNA complexes and transfection occurs while cells are attaching to the well.

In vitro migration/wound healing assays. Cells were seeded on an Ibidi single-culture insert (Ibidi GmbH, Munich, DE) in a 35 mm μ-dish, consists of two reservoirs separated by a 500 μm thick wall. Such inserts create a linear gap by adhering to the treated dish bottom and preventing cell growth in a predefined region. For the myoblasts migration assay an equal number of cells (3×10^4) were seeded in GM into the two reservoirs of the same insert and incubated at 37°C and 5% CO_2 until their attachment. After 12 hours, cells were treated for 2 hours with mytomicin (15 μg/mL; Sigma-Aldrich) to prevent proliferation. Subsequently, the insert was gently removed creating a gap of ~500 μm and the plate was filled with GM supplemented with different obestatin concentrations. The progress of migration was

photographed immediately, 8 and 24 hours after removing the reservoirs, near the crossing point. Unless indicated otherwise, obestatin was used at a concentration of 10 nM in scratch assays. The wound was calculated by tracing along the border of the scratch using the ImageJ64 analysis software and using the following equation: percentage of wound closure = [(wound area (0h)-wound area (xh))/wound area (0h)] x 100 (35).

Histology and immunofluorescence analysis. Muscle samples were prepared as described previously (36). Immunostaining analyses of grafted TA muscles were performed using mouse monoclonal antibodies specific for human spectrin and human Lamin A/C. These antibodies were used to visualize fibers expressing human proteins (anti-spectrin) and to detect human nuclei (anti-Lamin A/C). To evaluate the proliferation and differentiation of human cells during regeneration, double immunofluorescence analyses were performed combining antibodies directed against human Lamin A/C with the following antibodies: anti-Ki67 (a pan marker for cells within the cell cycle), anti-phosphohistone H3 (pH3; a marker of the M phase of cell cycle), and anti-myogenin (a marker of the early phase of myoblast differentiation). To evaluate the apoptosis of human cells, immunofluorescence analyses were performed using anti-Lamin A/C antibody and a terminal deoxynucleotidyl transferase dUTP nick end-labeling (TUNEL) assay (TACS® TdT In Situ Apoptosis Detection Kit-Fluorescein; R&D Systems, Minneapolis, MN). The nuclei of cells were further counter-stained with DAPI. The number of TUNEL- and Lamin A/C-positive nuclei was counted in ten images from non-overlapping areas of each group. Furthermore, apoptosis was evaluated by immunofluorescence analyses combining antibodies directed against human Lamin A/C with anti-cleaved caspases-3. Staining for MHC, a global marker for early and full differentiation of myoblasts, was performed using the antibody anti-Mf20 (a pan MHC antibody recognizing all isoforms expressed in differentiated skeletal muscle) together with an anti-human Lamin A/C. In addition, we used the anti-Pax7 antibody to detect satellite cells in the muscle tissue together with anti-human Lamin A/C and anti-laminin antibodies. General characteristics of all antibodies are summarized in Table S1. DAPI was used to counterstain nuclei (Life Technologies). The digital images of the

cell cultures were acquired with a Leica TCS-SP8 spectral confocal microscope (Leica Microsystems, Heidelberg, DE). Muscles were analyzed as previously described (58). Briefly, TA muscles were entirely cut into 5 µm sections. For every 450 µm along the complete length of the muscle, 10 sections corresponding to a 50 µm length were used for quantitative analyses. The number of spectrin-positive profiles in each section examined was counted and the maximum value was determined for each TA investigated. To quantify mononucleated interstitial Lamin A/C positive cells, three of the 10 sections analyzed, each separated by at least 15 µm, were assessed and the mean number of Lamin A/C positive cells was calculated. Finally, the mean value of Lamin A/C positive cells was calculated for all of the slides examined covering the entire length of the TA muscle.

Immunoblot analysis. The cell samples were directly lysed in ice-cold RIPA buffer [50 mmol/L Tris–HCl (pH 7.2), 150 mmol/L NaCl, 1 mmol/L EDTA, 1% (v/v) NP-40, 0.25% (w/v) Na-deoxycholate, protease inhibitor cocktail (Sigma Chemical), phosphatase inhibitor cocktail (Sigma-Aldrich)]. The lysates were clarified by centrifugation (14,000 ×g for 15 minutes at 4 °C) and the protein concentration was quantified using the QuantiProTM BCA assay kit (Sigma Chemical). For immunoblotting, equal amounts of protein were fractionated by SDS-PAGE and transferred onto nitrocellulose membranes. Immunoreactive bands were detected by enhanced chemiluminescence (Pierce ECL Western Blotting Substrate; Thermo Fisher Scientific, Pierce, Rockford, IL).

Statistical analysis. All values are presented as mean ± SEM. Statistical analyses were performed using Graph Pad Prism (version 5.0b; Graph Pad Software, San Diego, CA). Statistical significance was assessed by one-way ANOVA with the Bonferroni post-test or Student's unpaired t-test, with $P < 0.05$ being considered significant (*).

ACKNOWLEDGMENTS

REFERENCES

1. Negroni E, Bigot A, Butler-Browne GS, Trollet C, Mouly V (2016) Cellular Therapies for Muscular Dystrophies: Frustrations and Clinical Successes. *Hum Gene Ther* **27**: 117-126

2. Guiraud S, Aartsma-Rus A, Vieira NM, Davies KE, van Ommen GJ, Kunkel LM (2015) The Pathogenesis and Therapy of Muscular Dystrophies. *Annu Rev Genomics Hum Genet* **16**: 281-308

3. Maffioletti SM, Noviello M, English K, Tedesco FS (2014) Stem cell transplantation for muscular dystrophy: the challenge of immune response. *Biomed Res Int* 2014: 964010

4. Benedetti S, Hoshiya H, Tedesco FS (2013) Repair or replace? Exploiting novel gene and cell therapy strategies for muscular dystrophies. *FEBS J* **280**: 4263-4280

5. Bareja A, Billin AN (2013) Satellite cell therapy-from mice to men. *Skelet Muscle* **3**: 2

6. Bentzinger CF, Wang YX, von Maltzahn J, Rudnicki MA (2012) The emerging biology of muscle stem cells: implications for cell-based therapies. *Bioessays* **35**: 231–241

7. Watt DJ, Lambert K, Morgan JE, Partridge TA, Sloper JC (1982) Incorporation of donor muscle precursor cells into an area of muscle regeneration in the host mouse. *J Neurol Sci* **57**: 319–331

8. Partridge TA, Morgan JE, Coulton GR, Hoffman EP, Kunkel LM (1989) Conversion of mdx myofibres from dystrophin-negative to -positive by injection of normal myoblasts. *Nature* **337**: 176–179

9. Morgan JE, Hoffman EP, Partridge TA (1990) Normal myogenic cells from newborn mice restore normal histology to degenerating muscles of the mdx mouse. *J Cell Biol* 111: 2437-2449

10. Kinoshita I, Huard J, Tremblay JP (1994) Utilization of myoblasts from transgenic mice to evaluate the efficacy of myoblast transplantation. *Muscle Nerve* **17**: 975-980

11. Huard J, Tremblay G, Verreault S, Labrecque C, Tremblay JP (1993) Utilization of an antibody specific for human dystrophin to follow myoblast transplantation in nude mice. *Cell Transplant* **2**:113-118

12. Huard J, Verreault S, Roy R, Tremblay M, Tremblay JP (1994) High efficiency of muscle regeneration after human myoblast clone transplantation in SCID mice. *J Clin Invest* **93**: 586-599

13. Asselin I, Tremblay M, Vilquin JT, Gu.rette B, Roy R, Tremblay, JP (1995) Quantification of normal dystrophin mRNA following myoblast transplantation in mdx mice. *Muscle Nerve* **18**: 980–986

14. Huard J, Bouchard JP, Roy R, Labrecque C, Dansereau G, Lemieux B, Tremblay JP (1991) Myoblast transplantation produced dystrophin-positive muscle fibres in a 16-year-old patient with Duchenne muscular dystrophy. *Clin Sci* **81**: 287–288

15. Gussoni E, Pavlath GK, Lanctot AM, Sharma KR, Miller RG, Steinman L, Blau HM (1992) Normal dystrophin transcripts detected in Duchenne muscular dystrophy patients after myoblast transplantation. *Nature* **356**: 435–438.

16. Tremblay JP, Malouin F, Roy R, Huard J, Bouchard JP, Satoh A, Richards CL (1993) Results of a triple blind clinical study of myoblast transplantations without immunosuppressive treatment in young boys with Duchenne muscular dystrophy. *Cell Transplant* **2**: 99–112

17. Beauchamp JR, Morgan JE, Pagel CN, Partridge, TA (1999) Dynamics of myoblast transplantation reveal a discrete minority of precursors with stem cell-like properties as the myogenic source. *J Cell Biol* **144**: 1113–1122

18. Skuk D, Caron NJ, Goulet M, Roy B, Tremblay JP (2003) Resetting the problem of cell death following muscle-derived cell transplantation: detection, dynamics and mechanisms. *J Neuropathol Exp Neurol* **62**: 951–967.

19. Guérette B, Skuk D, Célestin F, Huard C, Tardif F, Asselin I (1997) Prevention by anti-LFA-1 of acute myoblast death following transplantation. *J Immunol* **159**: 2522–2531.

20. Morgan JE, Pagel CN, Sherratt T, Partridge TA (1993) Long-term persistence and migration of myogenic cells injected into pre-irradiated muscles of mdx mice. *J Neurol Sci* **115**:191-200

21. Skuk D, Goulet M, Tremblay JP (2011) Transplanted myoblasts can migrate several millimeters to fuse with damaged myofibers in nonhuman primate skeletal muscle. *J Neuropathol Exp Neurol* **70**:770–778

22. Skuk D, Goulet M, Tremblay JP (2013) Electroporation as a method to induce myofiber regeneration and increase the engraftment of myogenic cells in skeletal muscles of primates. *J Neuropathol Exp* Neurol **72** : 723–734.

23. Goetsch KP, Myburgh KH, Niesler CU (2013) In vitro myoblast motility models: investigating migration dynamics for the study of skeletal muscle repair. *J Muscle Res Cell Motil* **34**: 333–347

24. Skuk D, Goulet M, Roy B, Chapdelaine P, Bouchard JP, Roy R, Dugré FJ, Sylvain M, Lachance JG, Deschênes L, Senay H, Tremblay JP (2006) Dystrophin expression in muscles of duchenne muscular dystrophy patients after high-density injections of normal myogenic cells. *J Neuropathol Exp Neurol* **65**: 371–386.

25. Skuk D, Goulet M, Roy B, Piette V, Cote CH, Chapdelaine P, Hogrel JY, Paradis M, Bouchard JP, Sylvain M, Lachance JG, Tremblay JP (2007) First test of a "high-density injection" protocol for myogenic cell transplantation throughout large volumes of muscles in a Duchenne muscular dystrophy patient: eighteen monthsfollow-up. *Neuromuscul Disord* **17**: 38–46

26. Périé S, Trollet C, Mouly V, Vanneaux V, Mamchaoui K, Bouazza B, Marolleau JP, Laforêt P, Chapon F, Eymard B, Butler-Browne G, Larghero J, St Guily JL (2014) Autologous myoblast transplantation for oculopharyngeal muscular dystrophy: a phase I/IIa clinical study. *Mol Ther* **22**:219-25.

27. Yin H, Price F, Rudnicki MA (2013) Satellite Cells and the Muscle Stem Cell Niche. *Physiol Rev* **93**: 23–67

28. Cerletti M, Jurga S, Witczak CA, Hirshman MF, Shadrach JL, Goodyear LJ, Wagers AJ (2008) Highly efficient, functional engraftment of skeletal muscle stem cells in dystrophic muscles. *Cell* **134**: 37-47

29. Sacco A, Doyonnas R, Kraft P, Vitorovic S, Blau HM (2008) Self-renewal and expansion of single transplanted muscle stem cells. *Nature* 456:502-506

30. Tanaka KK, Hall JK, Troy AA, Cornelison DD, Majka SM, Olwin BB (2009) Syndecan-4-expressing muscle progenitor cells in the SP engraft as satellite cells during muscle regeneration. *Cell Stem Cell* **4**: 217-225

31. Collins CA, Olsen I, Zammit PS, Heslop L, Petrie A, Partridge TA, Morgan JE (2005) Stem cell function, self-renewal, and behavioral heterogeneity of cells from the adult muscle satellite cell niche. *Cell* **122**: 289-301

32. Riederer I, Negroni E, Bencze M, Wolff A, Aamiri A, Di Santo JP, Silva-Barbosa SD, Butler-Browne G, Savino W, Mouly V (2012) Slowing down differentiation of engrafted human myoblasts into immunodeficient mice correlates with increased proliferation and migration. *Mol Ther* **20**: 146-54

33. Charville GW, Cheung TH, Yoo B, Santos PJ, Lee GK, Shrager JB, Rando TA (2015) Ex Vivo Expansion and In Vivo Self-Renewal of Human Muscle Stem Cells. *Stem Cell Reports* **5**: 621-32

34. Bentzinger CF, von Maltzahn J, Dumont NA, Stark DA, Wang YX, Nhan K, Frenette J, Cornelison DD, Rudnicki MA (2014) Wnt7a stimulates myogenic stem cell motility and engraftment resulting in improved muscle strength. *J Cell Biol* **205**: 97-111.

35. Gurriarán-Rodríguez U, Santos-Zas I, Al-Massadi O, Mosteiro CS, Beiroa D, Nogueiras R, Crujeiras AB, Seoane LM, Señarís J, García-Caballero T, Gallego R, Casanueva FF, Pazos Y, Camiña JP (2012) The obestatin/GPR39 system is up-regulated by muscle injury and functions as an autocrine regenerative system. *J Biol Chem* **287**: 38379-3889

36. Gurriarán-Rodríguez U, Santos-Zas I, González-Sánchez J, Beiroa D, Moresi V, Mosteiro CS, Lin W, Viñuela JE, Señarís J, García-Caballero T, Casanueva FF, Nogueiras R, Gallego R, Renaud JM, Adamo S, Pazos Y, Camiña JP (2015) Action of obestatin in skeletal muscle repair: stem cell expansion, muscle growth, and microenvironment remodeling. Mol Ther **23**: 1003-1021

37. Santos-Zas I, Gurriarán-Rodríguez U, Cid-Díaz T, Figueroa G, González-Sánchez J, Bouzo-Lorenzo M, Mosteiro CS, Señarís J, Casanueva FF, Casabiell X, Gallego R, Pazos Y, Mouly V, Camiña JP (2016) β-Arrestin scaffolds and signaling elements essential for the obestatin/GPR39 system that determine the myogenic program in human myoblast cells. *Cell Mol Life Sci* **73**: 617-635.

38. Mamchaoui K, Trollet C, Bigot A, Negroni E, Chaouch S, Wolff A, Kandalla PK, Marie S, Di Santo J, St Guily JL, Muntoni F, Kim J, Philippi S, Spuler S, Levy N, Blumen SC, Voit T, Wright WE, Aamiri A, Butler-Browne G, Mouly V (2011) Immortalized pathological human

myoblasts, towards a universal tool for the study of neuromuscular disorders. *Skelet Muscle* **1**: 34

39. Bigot A, Jacquemin V, Debacq-Chainiaux F, Butler-Browne GS, Toussain, O, Furling D, Mouly V (2008) Replicative aging down-regulates the myogenic regulatory factors in human myoblasts. *Biol Cell* **100**: 189–199

40. Francis-West PH, Antoni L, Anakwe K (2003) Regulation of myogenic differentiation in the developing limb bud. *J Anat* **202**: 69–81

41. Skuk D, Tremblay JP (2015) Cell therapy in muscular dystrophies: many promises in mice and dogs, few facts in patients. *Expert Opin Biol Ther* **15**: 1307-1319

42. Blaveri K, Heslop L, Yu DS, Rosenblatt JD, Gross JG, Partridge TA, Morgan JE (1999) Patterns of repair of dystrophic mouse muscle: studies on isolated fibers. *Dev Dyn* **216**: 244–256

43. Heslop L, Beauchamp JR, Tajbakhsh S, Buckingham ME, Partridge TA, Zammit PS (2001) Transplanted primary neonatal myoblasts can give rise to functional satellite cells as identified using the Myf5nlacZ/+ mouse. *Gene Ther* **8**: 778–783

44. Day K, Shefer G, Richardson JB, Enikolopov G, Yablonka-Reuveni Z (2007) Nestin-GFP reporter expression defines the quiescent state of skeletal muscle satellite cells. *Dev Biol* **304**: 246-259

45. Halevy O, Piestun Y, Allouh MZ, Rosser BW, Rinkevich Y, Reshef R, Rozenboim I, Wleklinski-Lee M, Yablonka-Reuveni Z (2004) Pattern of Pax7 expression during myogenesis in the posthatch chicken establishes a model for satellite cell differentiation and renewal. *Dev Dyn* **231**: 489–502

46. Zammit PS, Golding JP, Nagata Y, Hudon V, Partridge TA, Beauchamp JR (2004) Muscle satellite cells adopt divergent fates: a mechanism for self-renewal? *J Cell Biol* **166**: 347–357

47. Wallingford JB, Habas R (2005) The developmental biology of Dishevelled: an enigmatic protein governing cell fate and cell polarity. *Development* **132**: 4421–4436

48. Gao C, Chen YG (2010) Dishevelled: The hub of Wnt signaling. *Cell Signal* **22**: 717-727

49. Glass DJ (2005) Skeletal muscle hypertrophy and atrophy signaling pathways. *Int J Biochem Cell Biol* **37**: 1974–1984

50. Lee CH, Inoki K, Guan KL (2007) mTOR pathway as a target in tissue hypertrophy. *Annu Rev Pharmacol Toxicol* **47**: 443–467

51. Egerman MA, Glass DJ (2014) Signaling pathways controlling skeletal muscle mass. *Crit Rev Biochem Mol Biol* **49**: 59-68

52. Alén BO, Nieto L, Gurriarán-Rodríguez U, Mosteiro CS, Álvarez-Pérez JC, Otero-Alén M, Camiña JP, Gallego R, García-Caballero T, Martín-Pastor M, Casanueva FF, Jiménez-Barbero J, Pazos Y (2012) The NMR structure of human obestatin in membrane-like environments: insights into the structure-bioactivity relationship of obestatin. *PLoS One* **7**: e45434

53. Gross JG, Morgan JE (1999) Muscle precursor cells injected into irradiated mdx mouse muscle persist after serial injury. *Muscle Nerve* **22**: 174–185

54. Heslop L, Beauchamp JR, Tajbakhsh S, Buckingham ME, Partridge TA, Zammit PS (2001) Transplanted primary neonatal myoblasts can give rise to functional satellite cells as identified using the Myf5nlacZl+ mouse. *Gene Ther* **8**: 778–783 |

55. Brimah K, Ehrhardt J, Mouly V, Butler-Browne GS, Partridge TA, Morgan JE (2004) Human muscle precursor cell regeneration in the mouse host is enhanced by growth factors. *Hum Gene Ther* **15**: 1109–1124

56. Cousins JC, Woodward KJ, Gross JG, Partridge TA, Morgan JE (2004) Regeneration of skeletal muscle from transplanted immortalised myoblasts is oligoclonal. *J Cell Sci* **117**: 3259–3269

57. Ehrhardt J, Brimah K, Adkin C, Partridge T, Morgan J (2007) Human muscle precursor cells give rise to functional satellite cells in vivo. *Neuromuscul Disord* **17**: 631–638

58. Negroni E1, Riederer I, Chaouch S, Belicchi M, Razini P, Di Santo J, Torrente Y, Butler-Browne GS, Mouly V (2009) In vivo myogenic potential of human CD133+ muscle-derived stem cells: a quantitative study. *Mol Ther* **17**: 1771–1778

59. Xiaoyin Xu, Zhong Yang, Qiang Liu and Yaming Wang (2010) In vivo Fluorescence Imaging of Muscle Cell Regeneration by Transplanted EGFP-labeled Myoblasts. *Mol Ther* **4**: 835–842

60. Vosshenrich CA, Ranson T, Samson SI, Corcuff E, Colucci F, Rosmaraki EE, Di Santo JP (2005) Roles for common cytokine receptor gamma-chain-dependent cytokines in the

generation, differentiation, and maturation of NK cell precursors and peripheral NK cells in vivo. *J Immunol* **174**: 1213–1221

61. Edom F, Mouly V, Barbet JP, Fiszman MY, Butler-Browne GS (1994) Clones of human satellite cells can express in vitro both fast and slow myosin heavy chains. *Dev Biol* **164**: 219–229

62. Kaufman SJ, Foster RF (1988) Replicating myoblasts express a muscle-specific phenotype. *Proc Natl Acad Sci USA* **85**: 9606–9610

63. Silva-Barbosa SD, Butler-Browne GS, Di Santo JP, Mouly V (2005) Comparative analysis of genetically engineered immunodeficient mouse strains as recipients for human myoblast transplantation. *Cell Transplant* **14**: 457–467

64. Decary S, Mouly V, Hamida CB, Sautet A, Barbet JP, Butler-Browne GS (1997) Replicative potential and telomere length in human skeletal muscle: implications for satellite cell-mediated gene therapy. *Hum Gene Ther* **8**: 1429–1438

FIGURE LEGENDS

Figure 1 Obestatin activates human myoblast proliferation in regenerating muscle. (**a**) Experimental scheme for the *in vivo* assay. Human myoblasts were isolated from the semitendinosus muscle of a 25-year-old male and implanted into the TA muscles of Rag2$^{-/-}$IL2Rb$^{-/-}$ mice immediately after cryodamage. Obestatin (300 nmol/Kg in DMEM) or vehicle (DMEM) was administrated via injection into the target muscles every 24 hours up to 5 consecutive days. At 24 hours, 5 and 21 days after engraftment, mice were sacrificed and the TAs were dissected. (**b**) Proliferation of human cells after injection into tibialis anterior (TA) muscles of Rag2$^{-/-}$IL2Rb$^{-/-}$ mice. *Upper panel*, quantification of Ki67$^+$ cells double-labeled with human specific anti-Lamin A/C antibody (human cells) is shown at 24 hours and 5 days post-injury after intramuscular injection of obestatin (300 nmol/kg body weight/24 hours during 5 days) or control (DMEM) following human myoblast transplantation (n=5 per group). Graph depicts percentage of human cell number that expressed Ki67. *Lower panel*, representative sample sections for Ki67 and Lamin A/C expression at 5 days following cell transplantation. (**c**) *Upper panel*, detection of phospho-hitone 3 (pH3) cells double-labeled with he human specific anti-Lamin A/C antibody is shown at 24 hours and 5 days following cell transplantation and intramuscular injection of obestatin (300 nmol/kg body weight/24 hours during 5 days; n=5 per group) or control (DMEM; n=5 per group). Graph depicts percentage of human cell number that expressed pH3. *Lower panel*, representative detection of pH3 and Lamin A/C at 24 hours following human myoblast transplantation. (**d**) *Upper panel*, quantification of TUNEL-positive cells double-labeled with human specific anti-Lamin A/C antibody (human cells) is shown at 24 hours and 5 days post-injury after intramuscular injection of obestatin (300 nmol/kg body weight/24 hours during 5 days) or control (DMEM) following human myoblast transplantation (n=5 per group). Graph depicts average percent of TUNEL-positive human cells. *Lower*

panel, representative detection of Lamin A/C and TUNEL labeling at 5 days following human myoblast transplantation. (**e**) Representative detection of cleaved caspase-3 and Lamin A/C at 24 hours and 5 days following cell transplantation and intramuscular injection of obestatin (300 nmol/kg body weight/24 hours during 5 days; n=5 per group) or control (DMEM; n=5 per group). In b, c and d, data are expressed as mean ± SEM. *P < 0.05 versus control values.

Figure 2 Obestatin treatment increases cell migration *in vitro* and *in vivo*. (**a**) Quantification of the area occupied by transplanted cells was made at 24 hours, 5 and 21 days after intramuscular injection of obestatin (300 nmol/kg body weight/24 hours during 5 days; n=5 per group) or control (DMEM; n=5 per group). The area was estimated as the area occupied by human cells, Lamin A/C$^+$ cells, on transverse sections along the entire length of the muscle and expressed as total area (*left upper panel*), relative area (area/cell number; *right upper panel*) and cell number per unit area (μm^2; *left bottom panel*). Data represent mean ± SEM. *P < 0.05 versus control values. *Right bottom panel,* representative sample sections of the area occupied by human cells detected by anti-Lamin A/C at 21 days following human myoblast transplantation. (**b**) *In vitro* migration potential of human primary myoblasts (C25 cells). *Upper panel* shows representative images of myoblasts cells in GM (control) or GM+obestatin (10 nM) 24-hour after stimulation. *Botton panel*, wound closure was evaluated using the equation described under Experimental Procedures. Values are mean ± S.E. of three independent experiments. *P < 0.05 versus control values. (**c**) Effect of siRNA depletion of Dvl2 on *in vitro* migration of human immortalized myoblasts. Cells transfected with Dvl2 (si-Dvl2) or scrambled control (si-control) siRNA were seeded into IBIDI inserts. *Right panel* shows representative images of immortalized myoblasts under GM (control) or GM+obestatin (10 nM) 24-hour after stimulation. Wound closure was evaluated using the equation described in Material & Methods section. Expression of Dvl2 was evaluated by immunoblot (*left panel*) 24-hour after stimulation. Values are

mean ± SEM of three independent experiments. *$P < 0.05$ versus control values. (**d**) Rac1 and Rho activation assays in immortalized myoblasts in GM (control) or GM+obestatin (10 nM). Cells were either treated with a siRNA targeting Dvl2 (si-Dvl2) or with a scrambled control (si-control). Total Rac1 or Rho is shown as a loading control. Activation of Rac1 and Rho was expressed relative to control siRNA-transfected cells (n=3). Immunoblots are representative of three independent experiments. Data are expressed as the mean ± SEM obtained from intensity scans of independent experiments. *$P < 0.05$ versus control values.

Figure 3 Obestatin promotes differentiation of muscle precursors *in vivo*. Representative sections stained for myogenin (**a**) or MHC (**b**) after intramuscular injection of obestatin (300 nmol/kg body weight/24 hours during 5 days) or control (DMEM) at 5 days following human myoblast transplantation (n=5 per group). In **a**, the analysis of the myogenin$^+$ cells double-labeled with the human specific anti-Lamin A/C antibody is shown at 5 days following cell transplantation. In **b**, quantification of MHC$^+$ myofibers with centrally located human nuclei (Lamin A/C$^+$; regenerating myofibers) is shown at 5 days following cell transplantation. Additionally, cross-sectional area of regenerating fibers and the number of myonuclei per MHC$^+$ regenerating myofiber was evaluated. Data are expressed as mean ± SEM. *$P < 0.05$ versus control values.

Figure 4 Obestatin increase engraftment capacity of human myoblasts *in vivo*. (**a**) *Left panel,* representative sections stained for Lamin A/C after intramuscular injection of obestatin (300 nmol/kg body weight/24 hours during 5 days; n=5 per group) or control (DMEM) at 21 days following human myoblast transplantation. *Right panel*, analysis of the number of myofibers containing nuclei expressing Lamin A/C$^+$ cells and of the number of incorporated human cells into regenerated muscle fibers is shown at 21 days following cell transplantation. (**b**) *Left panel,* representative sections stained for human-specific spectrin and Lamin A/C at 21 days following human myoblast

transplantation. *Right panel* shows the analysis of spectrin[+] fibers and cross-sectional area of total, spectrin[-] and spectrin[+] fibers at 21 days following cell transplantation. (**c**) The frequency distribution of the spectrin[+] fiber cross-sectional area was evaluated 21 days following human myoblast transplantation. In **a** and **b**, data are expressed as mean ± SEM (n=5 per group). *P < 0.05 versus control values.

Figure 5 Obestatin regulates self-renewal and expansion of transplanted human muscle cells. *Upper panel*, representative sections stained for Lamin A/C and Pax7 after intramuscular injection of obestatin (300 nmol/kg body weight/24 hours during 5 days; n=5 per group) or control (DMEM) at 21 days following human myoblast transplantation. Human Lamin A/C/Pax7 double positive cells (Pax7^{+}/Lamin AC[+]) localized underneath the basal lamina of myofibers, i.e. satellite cells from human origin, are indicated with white arrowheads. Pax7^{+}/Lamin AC[+] nuclei localized at the periphery of the muscle fiber are indicated with orange arrowheads. Pax7 positive and Lamin A/C negative (Pax7^{+}/Lamin AC[-]) nuclei localized underneath the basal lamina of myofibers are indicated with yellow arrowheads. Pax7 negative and Lamin A/C positive (Pax7^{-}/Lamin AC[+]) nuclei localized underneath the basal lamina of myofibers are indicated with cyan arrowheads. *Bottom panel* shows quantification of the number of Pax7^{+} cells, Pax7^{+}/Lamin AC^{+} cells, the % of Pax7^{+}/Lamin AC^{+} cells underneath the basal lamina and the number of Pax7^{+}/Lamin AC^{-} cells normalized per 100 TA muscle fibers (n=5 per group). Data are expressed as mean ± SEM (n=5 per group). *P < 0.05 versus control values.

Figure S1 Validation of obestatin/GPR39 functionality in human primary myoblasts. (**a**) Immunocytochemical detection of obestatin and GPR39 in human primary myoblasts (**a1** and **a3**) and myotubes (**a2** and **a4**) (C25 cells). (**b**) Immunoblot analysis of the effect of obestatin (10 nM, 5 min) on the activation of Akt [pAkt(S473)], ERK1/2 [pERK1/2(T202/Y204)], p38 [pp38(Y182)], c-Jun [pc-Jun(S63) and

pJunD(S100)] and CAMKII [pCAMKII(T286): α, β and γ isoforms] in human primary myoblasts (C25 cells). (**c**) *Upper panel*, dose-response effect of obestatin (0.1–100 nM) in human primary myoblast (C25 cells) proliferation (48 h, n=5). Quantification of cell number was carried out by cell counting using desmin, marker for myoblasts, and Topro to counterstain nuclei (*lower panel*). (**d**) Effect of obestatin (10 nM) on differentiating human primary myoblasts (C25 cells). MHC expression was determined by immunoblot 6 days after stimulation (n=3). (**e**) *Left panel*, immunofluorescence detection of MHC in human primary myotubes in DM (control) or DM + obestatin (10 nM) 6 days after stimulation (n=6). DAPI was used to counterstain nuclei. *Right panel*, The extent of differentiation was evaluated by the MHC⁺ myotube area (*left upper panel*), fusion index (*right upper panel*) and the percentages of MHC⁺ myotubes containing the indicated numbers of nuclei (*bottom panel*). Data in **c, d** and **e** are expressed as mean ± SEM. *P < 0.05 versus control values.
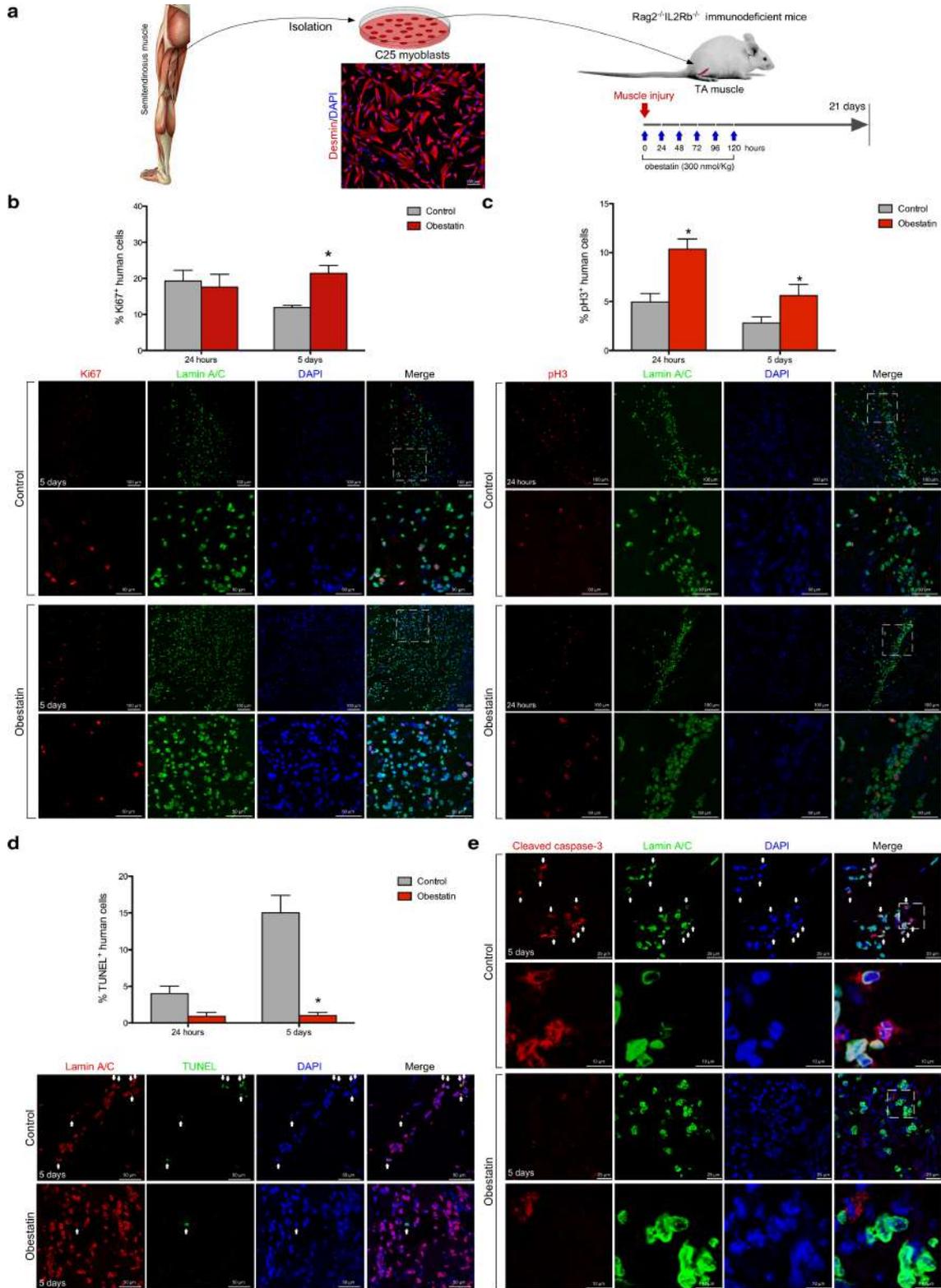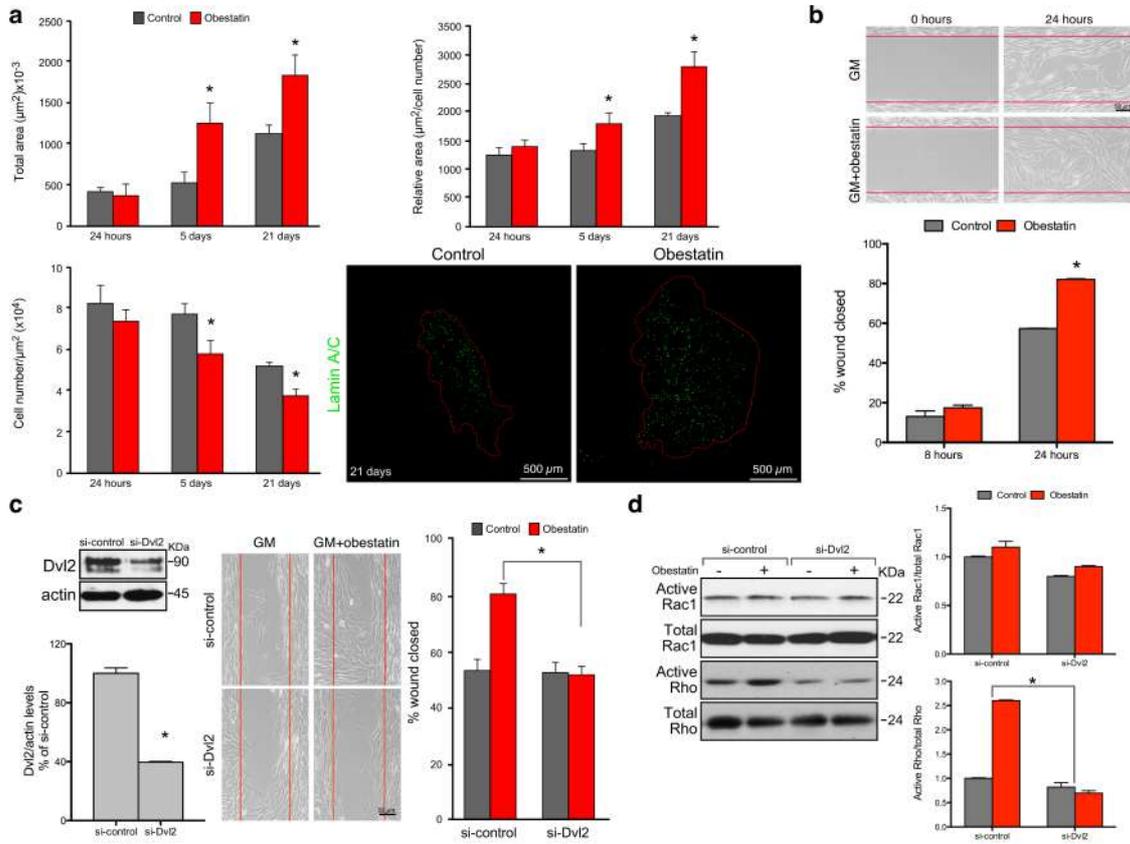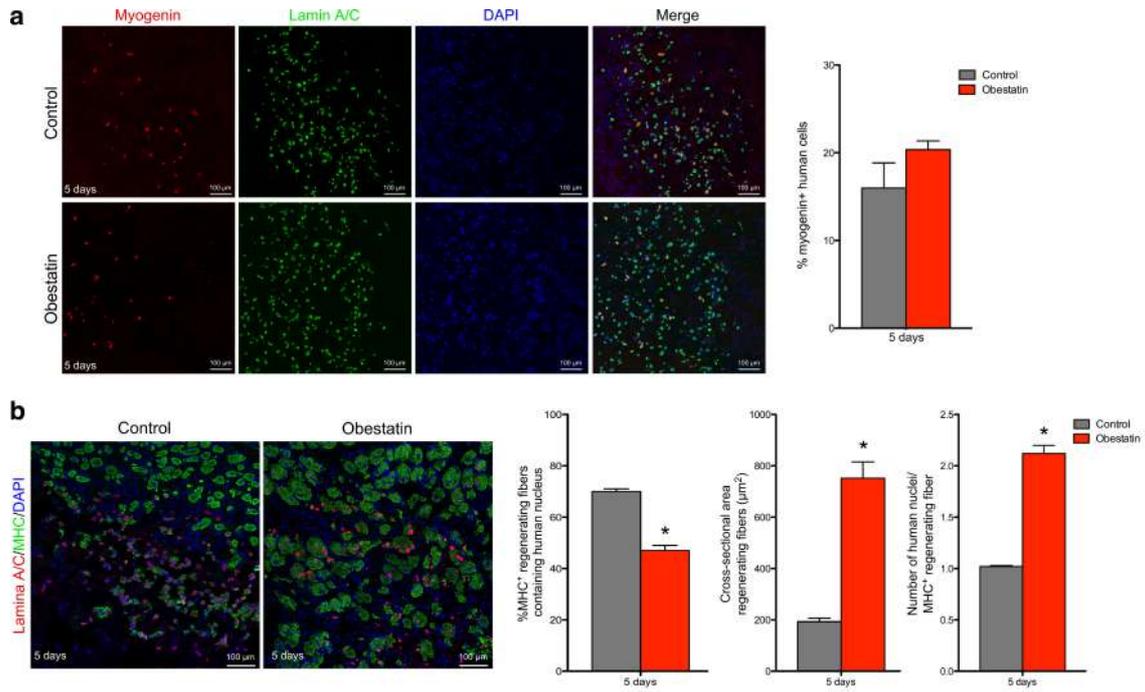
Figure 1

Figure 2

Figure 3

Figure 4

Figure 5

Figure S1